

Precision measurement of the magnetic field in terms of the free-proton NMR frequency

Xiang Fei*, V.W. Hughes, Ralf Prigl

Department of Physics, Yale University, New Haven, CT 06511, USA

Received 14 January 1997; received in revised form 26 March 1997

Abstract

We have developed a NMR standard probe using a spherical pure water sample of 1 cm diameter to determine the absolute magnetic field B in terms of the free-proton NMR frequency f_p with an accuracy of 3.4×10^{-8} . Our standard probe can be used conveniently to calibrate other probes in the field range from 1.45 to 1.7 T and can readily be employed over a much wider field range. The probe design and the tests carried out to verify its precision and accuracy are presented.

1. Introduction

Many experiments in metrology, atomic, nuclear and particle physics require an accurate determination of the spin precession frequency f_p of a free-proton in a magnetic flux density B

$$f_p = \left(\frac{\gamma_p}{2\pi} \right) B, \quad (1)$$

where γ_p is the free-proton gyromagnetic ratio. In two high-precision experiments currently in progress – the Brookhaven National Laboratory (BNL) muon g-2 experiment [1–3] and the Los Alamos (LAMPF) muonium ground-state spectroscopy experiment [4–6], the nuclear magnetic resonance (NMR) signals of protons in water samples are used for the magnetic field measurement [7]. In these experiments f_p has to be measured to an accuracy of 0.1 ppm, and hence, diamagnetic shielding of the protons in the sample and the susceptibility of the materials used for the NMR probes are important. The accuracy of the magnetic field value determined by Eq. (1) is currently limited by the knowledge of the proton gyromagnetic ratio (0.3 ppm) [8] in this work. In the latest CERN g-2 experiment corrections were applied to a standard probe which was then compared to the measurement probes used in the experiment and a calibration error of 0.6 ppm was quoted [9,10]. In the latest muonium precision spectroscopy experiment at LAMPF [11] the calibration error of the NMR probes was 0.3 ppm.

In a macroscopic substance containing protons, the magnetic field at the location of a proton B_p differs from the applied field B by an overall correction factor δ_t ,

$$B_p = (1 - \delta_t)B. \quad (2)$$

For a NMR probe with a water sample, the following effects contribute to δ_t : (1) Internal diamagnetic shielding in the water molecule, $\sigma(\text{H}_2\text{O})$, which depends slightly on temperature. (2) Bulk diamagnetism of the water sample which gives a contribution δ_b depending on the shape of the sample. (3) Paramagnetic impurities in the water sample, δ_p . (4) Paramagnetic and diamagnetic materials in the probe structure, δ_s . Hence

$$\delta_t = \sigma(\text{H}_2\text{O}) + \delta_b + \delta_p + \delta_s. \quad (3)$$

The dominant contribution to δ_t is the internal diamagnetic shielding $\sigma(\text{H}_2\text{O})$. For an atom or molecule the diamagnetic shielding arises from the Larmor precession of the electrons induced by the applied magnetic field B . For a hydrogen atom in its ground 1S state the shielding constant has been calculated [15,16] to be

$$\sigma(\text{H}) = \frac{\alpha^2}{3} \left(1 - \frac{1}{2} \frac{m}{M} \frac{3 + 4a_p}{1 + a_p} \right) = 17.733 \times 10^{-6}, \quad (4)$$

where α is the fine structure constant, m is the electron mass, M is the proton mass, and a_p is the proton magnetic moment anomaly. For a water molecule $\sigma(\text{H}_2\text{O})$ cannot be calculated accurately, but it has been determined from an experiment which compared the NMR frequency of a spherical pure water sample with the oscillation frequency of a

* Correspondence address: Indiana University Cyclotron Facility, Bloomington, IN 47408, USA. Tel.: +1 812 855 3598; fax: +1 812 855 6645; e-mail: fei@iucf.indiana.edu.

hydrogen maser in the same magnetic field [12,13], together with Eq. (4)

$$\sigma(\text{H}_2\text{O}, 34.7^\circ\text{C}) = 25.790(14) \times 10^{-6}. \quad (5)$$

In a separate experiment the temperature dependence of $\sigma(\text{H}_2\text{O})$ has been measured to be $10.36(30) \times 10^{-9}/^\circ\text{C}$ (from 5 to 45°C) [14].

The bulk diamagnetic shape correction is given by

$$\delta_b = (\varepsilon - 4\pi/3)\chi, \quad (6)$$

in which χ is the susceptibility and ε is a shape parameter. For a sphere $\varepsilon = 4\pi/3$ and therefore $\delta_b = 0$. For an infinitely long cylinder with its axis perpendicular to the magnetic field direction $\varepsilon = 2\pi$. For water $\chi(\text{H}_2\text{O}) = -0.720(2) \times 10^{-6}$ [17] and hence for a cylindrical probe $\delta_b = -1.508(4) \times 10^{-8}$, which means that the measured NMR frequency of a cylindrical probe is 1.51 ppm higher than that of a spherical probe in the same field. An air bubble distorts the shape of the water sample, so it is important to minimize the size of any air bubble in a spherical H_2O sample.

Usually paramagnetic ions are added to the water sample to reduce the proton spin relaxation time (T_1) which for pure water is about 3.5 s at room temperature [18]. This allows a higher repetition rate for successive field measurements but also causes a shift δ_p of the proton NMR frequency. For our standard probe, a short measurement time is not needed and a pure water sample with $\delta_p = 0$ has been used.

Since many NMR probes are involved in the experiments mentioned above, it is necessary to provide a carefully constructed standard NMR probe with high precision and accuracy for the calibration of these probes. We have designed and built a high-quality NMR probe with a spherical pure water sample. The probe design was checked first by mechanical and optical methods, and then tested in a 1.7 T field. In this paper, we discuss the design of the standard probe, describe the tests carried out to verify its precision and accuracy, and report a determination of the free-proton NMR frequency in a 1.7 T field to an accuracy of 3.4×10^{-8} .

2. Probe design and construction

General considerations for NMR probe design and radio frequency techniques can be found in Refs. [19,20]. Precision NMR probes are designed to minimize magnetic perturbations due to the probe structures and materials, and thus, only diamagnetic and weakly paramagnetic materials are used. A list of materials and their susceptibilities [21,22] is shown in Table 1. For a diamagnetic material χ is negative. The susceptibilities for the commonly used materials are about 10^{-6} .

Theoretical estimates for magnetic perturbations can be made [23], but it is also important to be able to measure them precisely. To a good approximation (distance to the field point much larger than the material dimension), a body

Table 1
Susceptibility χ for some commonly used materials

Substance	$\chi(10^{-6})$
Water	-0.72
Glass	-1.09
Copper	-0.76
Aluminum	+1.65
Silver	-1.90
Lead	-1.27
Teflon	-0.82

of volume V can be treated as having a magnetic dipole moment M which is proportional to its susceptibility, and the perturbation to the magnetic field B at a distance r in a plane perpendicular to the field is

$$\frac{\Delta B}{B} = \frac{M}{r^3} = \chi \frac{V}{r^3}. \quad (7)$$

For example, the shift caused by a body of 1 cm^3 volume and $\chi \sim 1 \times 10^{-6}$ is of the order of 10^{-9} at a distance of 10 cm. The effect is twice as large in the direction of the field, and hence, our probe is oriented perpendicular to the field to reduce the magnetic perturbation.

For a spherical shell or an infinitely long cylindrical tube of a uniformly distributed material with susceptibility $\chi \ll 10^{-4}$, the resulting relative change of the magnetic field inside is a second-order effect $\sim \chi^2 \ll 10^{-8}$ and therefore negligible. The end effect and the non-uniform distribution of materials should be measured and accounted for. As a design principle, the movable parts and irregular-shaped materials should be placed far from the sample while all parts close to the sample should have the geometry of a spherical shell or a cylindrical tube. A small distortion of the spherical sample holder leads to a shape correction which has been calculated for various spheroids using the formula in Ref. [24]. A fractional variation of 1% in the sample diameter causes a correction to δ_b of 2.4×10^{-8} .

Several spherical sample holders were fabricated from Pyrex glass by Wilmad Glass Company (Buena, New Jersey) with an inner diameter (ID) of 1.0 cm and an outer diameter (OD) of 1.1 cm. A cylindrical stem (neck), with 1 mm ID and 2 mm OD, is connected to it for easy handling and mechanical support. A long Teflon syringe needle of 0.79 mm OD and 0.33 mm ID is used for getting water in and out of the sample cell. The sphericity of the bulbs was checked with a Jones and Lamson (Model TC-14) optical comparator using a method similar to that described in Ref. [13]. In the process, a Pyrex glass bulb filled with water was immersed in a glycerol pool, images of the water sample or glass shape were magnified by a factor of 10, photographed, and then the sphericity of the glass bulb was measured from the photographs. Glycerol was used for matching the index of refraction of Pyrex glass. The

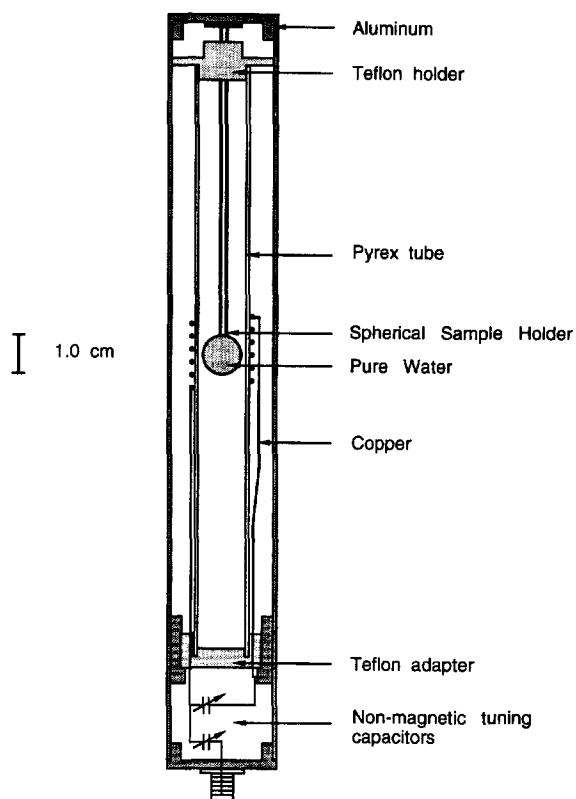


Fig. 1. NMR standard probe with a spherical water sample.

glycerol container was a polystyrene flask with parallel transparent walls (Corning Glass Works, 25110-75).

A schematic diagram of the standard probe is shown in Fig. 1. The upper portion of the glass neck is inserted in a Teflon holder and glued to it with “5 Minute” Epoxy (Devcon Corp.) to form the sample holder unit. The lower part of the Teflon piece can fit in the Pyrex tube with 13 mm ID and the upper part can be handled with fingers to get the unit in and out of the tube. The OD of the cylindrical tube is 15 mm and the copper coil is separated from the sample holder by this Pyrex tube to minimize its diamagnetic effect on the sample so that its influence is of the order of 0.01 ppm. The bottom of the cylindrical tube was glued to a Teflon adapter piece which is fixed to the aluminum case with screws to provide mechanical support and alignment for the sample holder. Small holes (2 mm diameter) were drilled in the Teflon adapter so the copper wires reach the capacitors underneath. A non-magnetic SMA connector is at the bottom of the probe for 50 Ω cable connection.

In our applications, the NMR probes are required to work at 1.45 T for the muon $g-2$ experiment and at 1.7 T for the LAMPF muonium experiment. Our design includes a frequency tuning feature which easily covers the field range from 1.45 to 1.7 corresponding to 61.7–72.4 MHz in proton NMR frequencies. The tuning circuit, shown in Fig. 2,

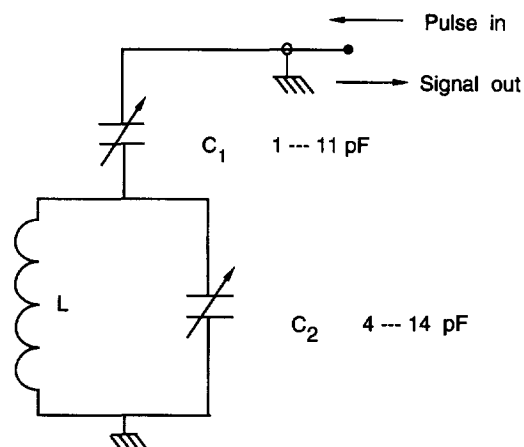


Fig. 2. NMR probe resonant circuit.

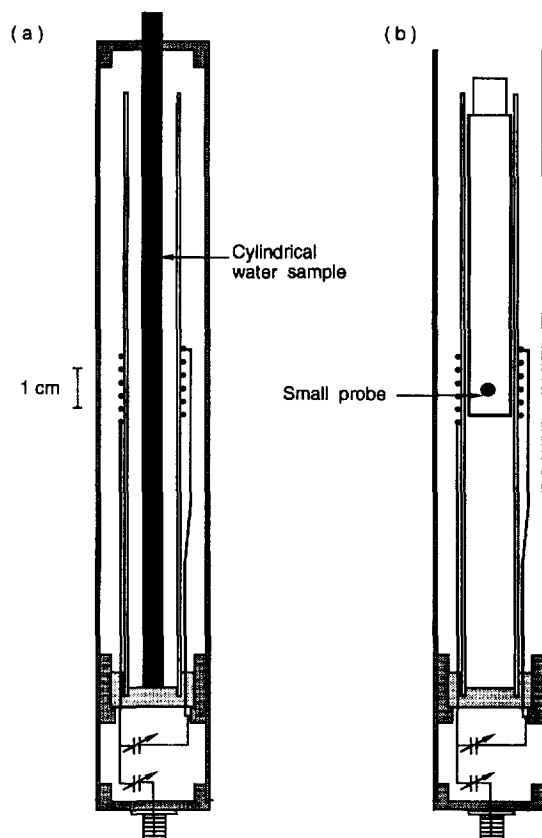


Fig. 3. Sample configurations: (a) a long cylindrical sample; (b) a small NMR probe.

consists of two non-magnetic variable capacitors C_1 and C_2 (Voltronics Corporation, Model NMKP10E), and a coil made of 5.5 turns of thin silver-plated copper wire (0.5 mm OD) with an inductance of about 0.6 μH . C_2 is used mainly to tune the resonance frequency of the NMR probe to match

the proton NMR frequency in the magnetic field and C_1 is used for the impedance match to $50\ \Omega$. Both capacitors are tuned in several iterations with a ceramic blade tool. Tuning employs a network analyzer and an impedance meter. Typical Q values are about 60. Since the two tuning capacitors are 8 cm from the water sample, the standard probe can work at various magnetic field values without introducing corrections associated with the tuning capacitors.

The probe is designed so that a long cylindrical sample (Fig. 3(a)) or a small NMR probe (Fig. 3(b)) can be inserted in place of the spherical water sample for systematic studies. One type of measurement probe has an outer diameter of 12 mm and can be inserted in the Pyrex tube of the standard probe replacing the spherical sample to measure the field perturbation caused by the standard probe case.

3. Experiment

We tested our precision NMR probes in the field of a large bore superconducting magnet operating in the persistent mode and having a high field stability and excellent homogeneity. The magnet is a conventional MRI magnet (Oxford Magnet Technology) and is being used at LAMPF for the muonium experiment [4–6]. The bore of the magnet is 1.05 m in diameter and 2.2 m in length. An iron shimming package, a set of electrical shimming coils and an additional modulation coil in the bore reduce the clear bore diameter to 70 cm, which is big enough for NMR test and calibration measurements.

The operating field is 1.7 T which corresponds to a proton spin precession frequency of 72 MHz. The field uniformity is better than 1 ppm over a 20 cm diameter spherical volume (DSV) and the drift rate in the persistent current mode at a constant temperature is less than 0.01 ppm/h after one week of operation. Ambient temperature fluctuations cause a slow field drift of up to 0.1 ppm/h, but the short-term stability of the field, which is about 0.001 ppm over seconds, was not affected.

A pulsed NMR magnetometer was developed [25] and tested [26] for high-precision magnetic field measurements. A short ($\sim 5\ \mu\text{s}$) 10 W RF excitation pulse is used. The Free Induction Decay (FID) signals picked up by the detection coil are amplified and then mixed with a known reference frequency which is 10–50 kHz lower than the signal frequency. The NMR measurement is carried out by counting the number of zero crossings of the low-frequency mixed FID signal in a well-measured time interval synchronized to the FID period. The NMR frequency is then calculated as the sum of the measured frequency and the reference frequency. On-line NMR data histograms are available in the computer memory at any time during the measurements. The FID signal can be recorded with an ADC and Fourier transformed to provide the NMR frequency, amplitude and line shape. This process is slower but useful for system tests and

systematic studies. Typically 25 NMR probes are operated with the magnetometer by multiplexing of the RF pulses and the signal detection. The minimum time interval between subsequent measurements is about 40 ms, and thus, each probe may be read out every second or even faster if less than 25 probes are used. Various types of probes smaller than the standard probe were used in the experiments and were calibrated. The typical FID time constant of the measurement probes is about 10 ms due to the field inhomogeneity produced by the probe materials and to the addition of paramagnetic salts. A complete report on the NMR magnetometer is given in Ref. [27].

Since absolute frequency measurement is essential, the frequency synthesizer used for providing the RF pulses and for mixing with the NMR frequency is frequency-locked to a LORAN-C receiver (Stanford Research Systems, Model FS700) which serves as a NIST traceable frequency standard with a long-time stability of 10^{-12} and a short-time stability of 10^{-10} .

An aluminum calibration platform was built to position NMR probes in the bore of the magnet. There are two ports separated by 20 cm for holding NMR probes on a sliding aluminum plate supported by the calibration platform. The vertical position of each port together with its NMR probe can be adjusted. The sliding plate can move back and forth along the magnetic field direction. In this way two probes can be located in turn at the center of the magnet where the field is shimmed to better than 10^{-8} in a 1 cm DSV and NMR frequency measurements of two probes can be compared in the same field.

In Fig. 4 the FID signal of the standard probe with the spherical water sample is shown. The signal has an approximately Gaussian envelope and decays with a time constant of 0.2 s. Its Fourier transform (FT) has a line width of 2 Hz (3×10^{-8}) which is largely due to the field inhomogeneity generated by the standard probe. When the spherical sample in the standard probe was replaced by a long cylindrical water sample (Fig. 3(a)) and a minor adjustment of the gradient field along the sample reduced the line width to 1 Hz (Fig. 5) by shimming away the gradient produced by the NMR probe.

The standard deviation of the short-term frequency measurement with the standard probe by the zero crossing method is the resolution of the magnetometer, which is typically 0.14 Hz or 2×10^{-9} . The zero crossing method and the FT method are consistent within 10^{-8} . In a typical run, two probes are moved back and forth so that each probe stays in the center for about 90 s during which time proton NMR frequencies are measured. The frequency differences for two probes at the same location are averaged to minimize the small field drift effect. Two probes were compared in many runs at different times and the result was repeatable to 10^{-8} . This is an indication that the calibration precision with the platform is about 10^{-8} . The effect on a reference probe when the standard probe was mounted on the other port was measured to be 3×10^{-9} . The exchange of NMR

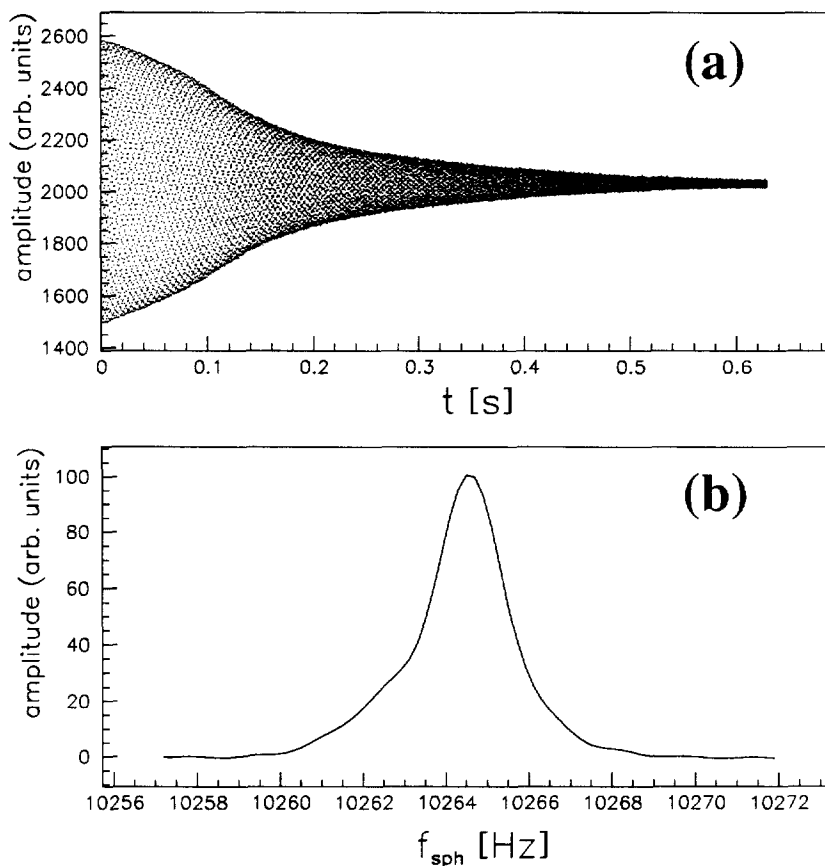


Fig. 4. NMR signals for the probe with a spherical water sample: (a) FID signal; (b) Fourier transform.

probes on the calibration platform is necessary. We also swapped probe A in port 1 with probe B in port 2 to study corrections arising from the fact that probes sense different magnetic fields at different ports due to a small asymmetry of the sliding plate. A difference of 10^{-8} was found. The average of the two configurations gives the final result.

Rotation tests for NMR probes were carried out to investigate the quality of the construction of the probes. Each NMR probe on the port can be rotated about its cylindrical axis and then compared to a reference probe. The changes due to the probe rotation are about 2×10^{-8} , which is an indication of the asymmetry of the probe. This effect is comparable to the line width of the FT signal.

A temperature difference between the probes in the two ports leads to an additional correction. We found that it took more than 20 min for the water samples in the probes to reach the ambient temperature in the center region of the magnet. The frequency drift due to the sample temperature change is dominated by the temperature dependence of about 0.01 ppm/K and was observed in our measurement. Probes were first put near the calibration platform for more than 30 min so that they reach the same temperature and then used for a comparison measurement.

The excitation/detection coil can change the magnetic field slightly due to the diamagnetic susceptibility of the copper wire. We wound copper wires (the same type of wire as used in the standard probes) on a probe to measure the frequency shift as a test of material influence. A piece of wire 4 times as long as the one used for the coil was wrapped around the aluminum case at the middle of the probe. A shift of 10^{-8} was observed.

In the probe configuration shown in Fig. 3(b), a measurement probe replaces the spherical sample holder unit and its NMR frequency is compared with a reference probe, as shown in Fig. 6. When the standard probe case (housing) is removed, the change of the differences is due to the standard probe case. We also deliberately moved the small probe vertically off-center by 3 mm and no frequency shift was observed. For the spherical and cylindrical probes, the NMR frequency shifts due to the probe cases were measured to be -1.8 Hz (2.5×10^{-9}) and -2.8 Hz (4×10^{-9}), respectively.

The inner diameter of the stem for the spherical probe is sufficiently small that the NMR frequency is insensitive to residual water in the stem or a tiny air bubble. The calculated correction due to the sample and its glass container

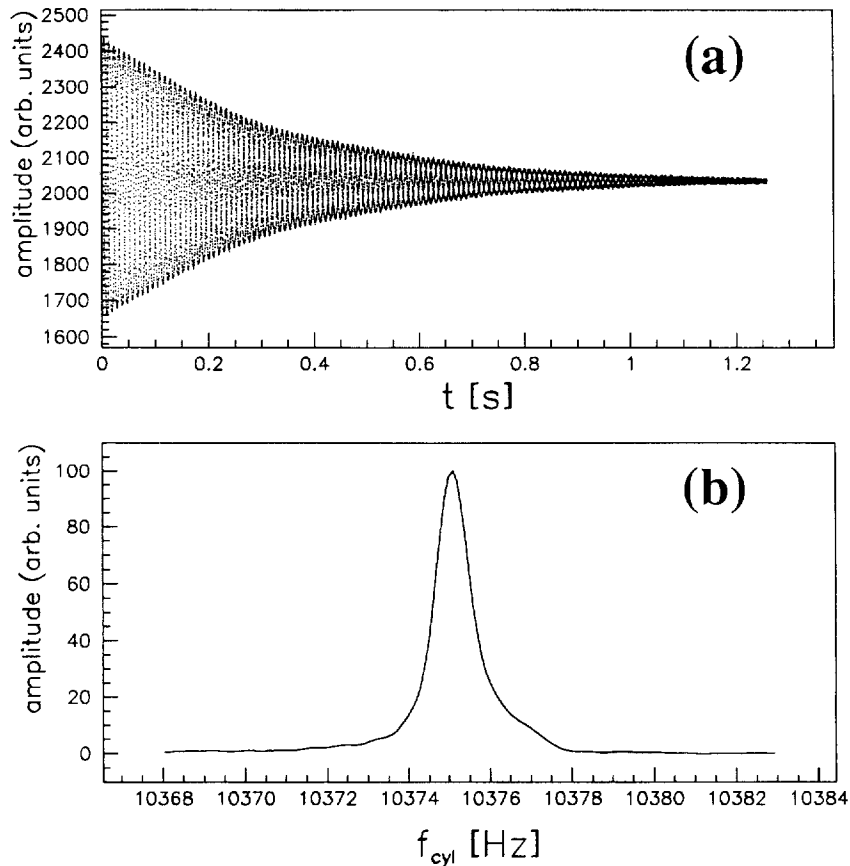


Fig. 5. NMR signals for the probe with a cylindrical water sample after shimming out the probe effect: (a) FID signal; (b) Fourier transform.

is -2×10^{-8} or -1.4 Hz based on observations by the optical comparator. The length of the water sample in the long cylindrical glass tube (Wilmad 535-pp-7) is 17.7 cm and the inner diameter is 0.42 cm. The length/diameter ratio is 42 which gives a correction of about -9×10^{-9} or -0.6 Hz. The overall shielding effects due to the probe body are: -3.2 Hz (-4.4×10^{-8}) for the spherical probe and -3.4 Hz (-4.7×10^{-8}) for the cylindrical probe.

As discussed in the Introduction, a fractional frequency difference between the NMR frequency f_{cyl} of a cylindrical sample and that of a spherical one, f_{sph} , is

$$\frac{\Delta f_p}{f_p} = \frac{f_{\text{cyl}} - f_{\text{sph}}}{f_p}(\text{theor}) = 1.508(4) \times 10^{-6}. \quad (8)$$

A careful comparison was made for the standard probe and a precision cylindrical probe, as shown in Fig. 7. The direct comparison gave a value 1.506 ppm. Taking into account the correction to compensate for probe differences established earlier (3×10^{-9})

$$\frac{f_{\text{cyl}} - f_{\text{sph}}}{f_p}(\text{expt}) = 1.509(10) \times 10^{-6} \quad (9)$$

Table 2

Error contributions

Source of error	Uncertainty
NMR detection and measurement	1.5×10^{-8}
Field homogeneity	1.0×10^{-8}
Materials outside the probe	1.5×10^{-8}
Water/sample holder shape	1.5×10^{-8}
Probe materials	1.0×10^{-8}
Diamagnetic shielding (H_2O)	1.4×10^{-8}
Temperature effect	1.0×10^{-8}
Total:	3.4×10^{-8}

which is in excellent agreement with Eq. (8). Alternatively, a value for the susceptibility of water of $\chi = -0.721(5) \times 10^{-6}$ can be deduced from our measurements, which agrees with a more precise value $-0.720(2) \times 10^{-6}$ [17].

The overall uncertainties in the experiment are summarized in Table 2. The NMR measurement error including the NMR spectrometer stability, field stability and experimenter influence when working near the magnet is 1.0×10^{-8} . Coupling between the proton oscillator and the detection

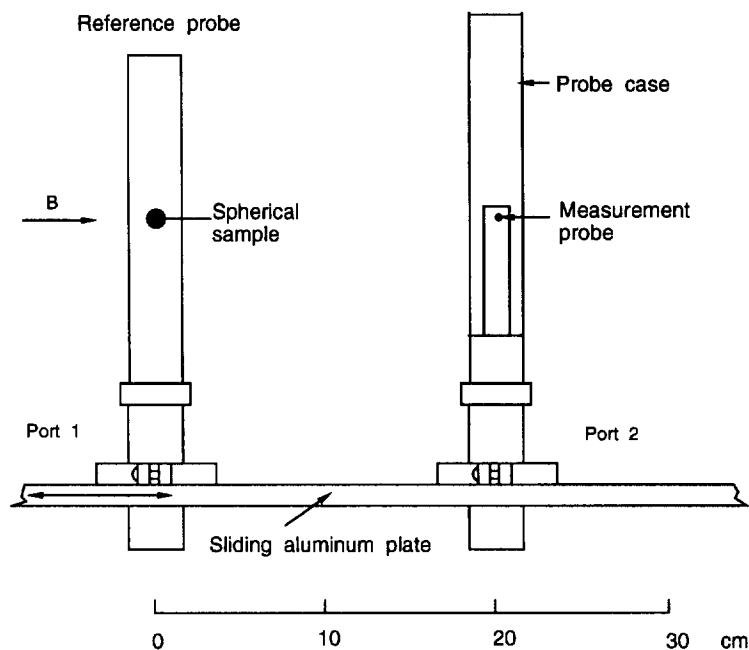


Fig. 6. Comparison of a measurement probe (with and without the standard probe case) with a reference probe. The change of the differences is due to the probe case.

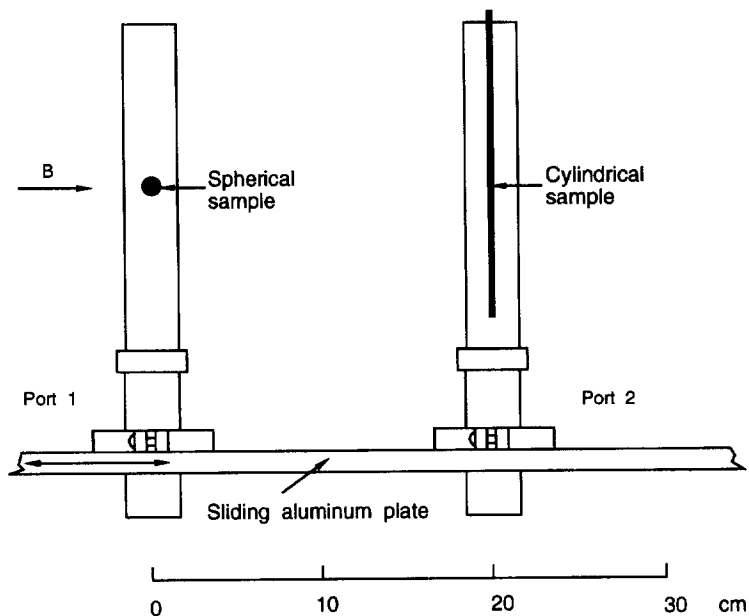


Fig. 7. Comparison of NMR probes with a spherical water sample and a cylindrical one in a calibration platform.

resonant circuit can cause a shift in the proton spin precession frequency. For our detection parameters and detuning, the pulling effect on f_p is estimated to be less than 10^{-8} . The effect of a probe at one port on a probe at the other port is about 10^{-9} , which is negligible. Additional errors come

from the diamagnetic shielding factor and the temperature effect and amount to 1.5×10^{-8} . The absolute free-proton spin precession frequency in the magnetic field B unperturbed by the presence of the measurement device (the standard probe) has an overall uncertainty of 3.4×10^{-8} .

4. Discussion

We have developed a standard probe containing a spherical water sample which has been used to measure magnetic fields in terms of the proton spin precession frequency. Using the known value for the diamagnetic shielding constant $\sigma(\text{H}_2\text{O})$ of protons in a spherical water sample, we thus measure the magnetic field in terms of the free-proton spin precession frequency to an accuracy of 3.4×10^{-8} . Since $f_p = \gamma_p B / 2\pi$ (Eq. (1)) and the gyromagnetic ratio of the proton in SI units $\gamma_p / 2\pi = 42.577469(13)$ MHz/T [8], the absolute value of the field can be given in T or G. Our standard probe can be operated in the field range from 1.45 to 1.7 T, which is adequate for absolute field calibration for the muon g-2 experiment at the BNL and for the muonium experiment at LAMPF, and a much wider field range is easily achievable. A further improvement in the precision measurement of the magnetic field in terms of the free-proton spin precession frequency requires a more precise value for the diamagnetic shielding factor of water which currently is known to 0.014 ppm. It is interesting to note that the ^3He nucleus serving as a NMR reference [7,17,28,29] has many merits for its low susceptibility, wide temperature range and simple symmetric line shape. Despite the experimental complexity for the optically pumped polarized helium-3 sample, it is very promising for precision magnetic field measurements [29].

Acknowledgements

It is a pleasure to thank W.D. Phillips, B.W. Petley, J.L. Flowers, B.N. Taylor, and E. Williams for informative suggestions. We thank W.M. Morse, F.J.M. Farley, G. zu Putnitz, and K. Jungmann for their interest. We are grateful to A. Disco for working on the calibration platform. We thank our colleagues at LAMPF and the machine shop in the Department of Physics at Yale University for their assistance. This work was supported in part by the U.S. Department of Energy, the Bundesminister fuer Forschung und Technologie of Germany, and the Alexander von Humboldt Foundation (for R.P.) from Germany.

References

- [1] V.W. Hughes et al., in: T. Hasegawa, N. Horikawa, A. Masaike and S. Sawada (Eds.), "The anomalous magnetic moment of the muon", *Frontiers of High Energy Spin Physics: Proc. of the 10th Int. Symp. on High Energy Spin Physics*, Universal Academy Press, Inc. Tokyo, Japan, 1993, pp. 717–722.
- [2] L. Roberts, in: K. Jungmann, V.W. Hughes, G. zu Putnitz (Eds.), *The Future of Muon Physics*, Springer, Berlin Heidelberg, 1992, p. 101.
- [3] V.W. Hughes, in: E.C.G. Sudarshan (Ed.), *Gift of Prophecy, Essays in Celebration in the Life of Robert Eugene Marshak*, World Scientific, Singapore, 1995, p. 222.
- [4] V.W. Hughes, G. zu Putnitz, in: T. Kinoshita (Ed.), *Quantum Electrodynamics*, World Scientific, Singapore, 1990, p. 822.
- [5] M.G. Boshier et al., in: M. Leon (Ed.), *Proc. Int. Workshop on Low Energy Muon Science*, LA-12698-C, LANL, Los Alamos, 1994, pp. 154–162.
- [6] M.G. Boshier et al., *Phys. Rev. A* 52 (1995) 1948.
- [7] X. Fei, V.W. Hughes, *Muon g-2 Technical Note* 131, Brookhaven National Laboratory, 1992.
- [8] E.R. Cohen, B.N. Taylor, *Rev. Mod. Phys.* 59 (1987) 1121.
- [9] K. Borer, F. Lange, *Nucl. Instr. and Meth.* 143 (1977) 219.
- [10] J. Bailey, et al., *Nucl. Phys. B* 150 (1979) 1.
- [11] F.G. Mariam, W. Beer, P.R. Bolton, P.O. Egan, C.J. Gardner, V.W. Hughes, D.C. Lu, P.A. Souder, H. Orth, J. Vetter, U. Moser, G. zu Putnitz, *Phys. Rev. Lett.* 49 (1982) 993.
- [12] W.D. Phillips, W.E. Cooke, D. Kleppner, *Phys. Rev. Lett.* 35 (1975) 1619.
- [13] W.D. Phillips, W.E. Cooke, D. Kleppner, *Metrologia* 13 (1977) 179.
- [14] B.W. Petley, R.W. Donaldson, *Metrologia* 20 (1984) 81.
- [15] W.E. Lamb, Jr., *Phys. Rev.* 60 (1941) 817.
- [16] H. Grotch, R.A. Hegstrom, *Phys. Rev. A* 4 (1971) 59.
- [17] Y.I. Neronov, A.E. Barzakh, *Sov. Phys. JETP* 48 (1978) 769.
- [18] J.H. Simpson, H.Y. Carr, *Phys. Rev.* 111 (1958) 1201.
- [19] E. Fukushima, S.B.W. Roeder, *Experimental Pulse NMR: A Nuts and Bolts Approach*, Addison-Wesley, Reading, MA., 1981.
- [20] R. Schetgen (Ed.), *The ARRL Handbook for Radio Amateurs*, The American Radio Relay League, Newington, CT, 1993.
- [21] R.C. Weast (Ed.), *CRC Handbook of Chemistry and Physics*, CRC Press, Boca Raton, 1986.
- [22] P.T. Keyser, S.R. Jefferts, *Rev. Sci. Instr.* 60 (1989) 2711.
- [23] J.D. Jackson, *Classical Electrodynamics*, Wiley, New York, 1975.
- [24] A.H. Morrish, *The Physical Principles of Magnetism*, J. Wiley, New York, 1965.
- [25] U. Haeblerlen, K. Jungmann, R. Prigl, G. zu Putnitz, P. van Walter, *Muon g-2 Technical Note* 78, Brookhaven National Laboratory, 1991.
- [26] R. Prigl, K. Jungmann, G. zu Putnitz, P. van Walter, U. Haeblerlen, X. Fei, V.W. Hughes, M. Janousch, W. Liu, W. Schwarz, *Muon g-2 Technical Note* 161, Brookhaven National Laboratory, 1993.
- [27] R. Prigl, U. Haeblerlen, K. Jungmann, G. zu Putnitz, P. von Walter, *Nucl. Instr. and Meth. A* 374 (1996) 118.
- [28] W.L. Williams, V.W. Hughes, *Phys. Rev.* 185 (1969) 1251.
- [29] J.L. Flowers, B.W. Petley, M.G. Richards, *Metrologia* 30 (1993) 75.